ACCELERATED COMMUNICATION

Backdoor opening mechanism in acetylcholinesterase based on X-ray crystallography and molecular dynamics simulations

Benoît Sanson,[1,2,3] Jacques-Philippe Colletier,[1,2,3,4] Yechun Xu,[4] P. Therese Lang,[5] Hualiang Jiang,[4,6] Israel Silman,[7] Joel L. Sussman,[8] and Martin Weik[1,2,3,9]*

[1]Comissariat à l'Energie Atomique, Institut de Biologie Structurale, F-38054 Grenoble, France
[2]CNRS, F-38027 Grenoble, France
[3]Université Joseph Fourier, F-38000 Grenoble, France
[4]Drug Discovery and Design Center, Shanghai Institute of Materia Medica, Chinese Academy of Sciences, Shanghai 201203, China
[5]Department of Molecular and Cell Biology, University of California, Berkeley, California 97420-3220
[6]School of Pharmacy, East China University of Science and Technology, Shanghai 200237, China
[7]Department of Neurobiology, Weizmann Institute of Science, Rehovot 76100, Israel
[8]Department of Structural Biology, Weizmann Institute of Science, Rehovot 76100, Israel
[9]European Synchrotron Radiation Facility, 6 rue Jules Horowitz, BP 220, 38043 Grenoble Cedex, France

Received 20 February 2011; Revised 6 May 2011; Accepted 6 May 2011
DOI: 10.1002/pro.661
Published online 18 May 2011 proteinscience.org

Abstract: The transient opening of a backdoor in the active-site wall of acetylcholinesterase, one of nature's most rapid enzymes, has been suggested to contribute to the efficient traffic of substrates and products. A crystal structure of *Torpedo californica* acetylcholinesterase in complex with the peripheral-site inhibitor aflatoxin is now presented, in which a tyrosine at the bottom of the active-site gorge rotates to create a 3.4-Å wide exit channel. Molecular dynamics simulations show that the opening can be further enlarged by movement of Trp84. The crystallographic and molecular dynamics simulation data thus point to the interface

Additional Supporting Information may be found in the online version of this article.

Benoît Sanson and Jacques-Philippe Colletier contributed equally to this work

Benoît Sanson's current address is Biology Department, Brookhaven National Laboratory, Upton, NY 11973-5000, USA.

Grant sponsors: CEA, the CNRS, and the UJF; Grant sponsor: Agence Nationale de la Recherche (ANR); Grant number: ANR-09-BLAN-0192-04; Grant sponsor: DGA; Grant number: DGA-REI 2009-34-0023; Grant sponsor: National Natural Science Foundation of China; Grant number: 31050110434; Grant sponsor: State Key Program of Basic Research of China; Grant number: 2009CB918501; Grant sponsor: Computer Network Information Center (CNIC) of the Chinese Academy of Sciences (CAS) and Shanghai Supercomputing Center (SCC) [for Computational resources (grant from the Information Construction Project of the CAS during the period of the 11th Five-Year Plan)].

*Correspondence to: Martin Weik, Comissariat à l'Energie Atomique, Institut de Biologie Structurale, F-38054 Grenoble, France. E-mail: weik@ibs.fr

between Tyr442 and Trp84 as the key element of a backdoor, whose opening permits rapid clearance of catalysis products from the active site. Furthermore, the crystal structure presented provides a novel template for rational design of inhibitors and reactivators, including anti-Alzheimer drugs and antidotes against organophosphate poisoning.

Keywords: acetylcholinesterase; X-ray crystallography; sub-domain; molecular dynamics simulations; substrate traffic; backdoor

Acetylcholinesterase (AChE) plays a crucial role at cholinergic synapses in both the central and peripheral nervous systems, terminating impulse transmission by rapid hydrolysis of the neurotransmitter acetylcholine.[1] AChE also attracts considerable interest in pharmacological, agrochemical, and toxicological contexts, being the target of a variety of natural and man-made drugs and inhibitors, such as organophosphate nerve agents and insecticides, the snake-venom polypeptide toxin, fasciculin, and the first generation of drugs for management of Alzheimer's disease. The first crystal structure of an AChE, that of *Torpedo californica* (*Tc*) AChE, revealed an unusual and unanticipated architecture[2] in view of its remarkably high catalytic power (turnover number 1000–10,000 s^{-1} depending on the species); the active site, a Ser-His-Glu catalytic triad, is buried at the bottom of a deep and narrow gorge. The crystal structure raised cogent questions as to how traffic of substrate and products to and from the active site might occur.[3] Molecular dynamics (MD) simulations indicated the presence of a backdoor in the thin aspect of the gorge, adjacent to the active site, which might permit transit of substrate, products, or solvent.[4–6] It was suggested that it might open transiently, in the course of catalysis, because of movement of residues within the ω-loop (residues 67–94 in *Tc*AChE). The residual catalytic activity observed in the complex of AChE with fasciculin, which almost completely blocks access to the active-site via the top of the gorge,[7] lent support to the backdoor hypothesis. Yet, extensive kinetic studies, together with site-directed mutagenesis,[8,9] failed to identify the backdoor, and X-ray crystallography, so far, has provided only circumstantial evidence for its existence.[10,11]

Here, we present a crystal structure of *Tc*AChE in complex with the inhibitor aflatoxin at 2.3 Å resolution, in which a large conformational change in the side chain of Tyr442 results in the opening of a backdoor [compare Fig. 1(A,B)], without involving residues within the ω-loop that had previously been the prime candidates.[4] The structure (PDB entry code 2XI4) was obtained after soaking orthorhombic crystals of native *Tc*AChE with aflatoxin (see Supporting Information), which binds to the peripheral anionic site (PAS), located at the top of the gorge, about 13 Å distant from the active site (Sanson *et al.*, unpublished). Bound aflatoxin is observed in both monomers of the dimer that constitutes the asymmetric unit of orthorhombic crystals of *Tc*AChE (not shown). In the native structure (PDB entry code 1W75), Tyr442Oζ H-bonds to Trp84Nε1 (distance 3.2 Å), linking the two subdomains of *Tc*AChE (residues 4–305 and 306–535) across the active-site gorge,[12] and the backdoor is closed [Fig. 1(C)]. In the complex, rotation of Tyr442 occurs in monomer A [Fig.1(D) and Supporting Information Fig. S1(A)], but not in monomer B [Supporting Information Fig. S1(B)], breaking the H-bond linking Tyr442Oζ to Trp84Nε1 (new distance, 12.7 Å); this results in the opening of a channel between the active site and the exterior large enough to allow the passage of a water molecule [Fig. 1(B)]. The structural environments of monomers A and B in the crystal are identical, and aflatoxin binding occurs in both monomers; hence, it is unclear why Tyr442 undergoes a conformational change only in monomer A. Small variations in the conformational heterogeneity of both monomers that are not detectable by X-ray crystallography may be at the origin of the differential behavior of Tyr442. Rotation of Tyr442 in monomer A also disrupts the H-bond linking Tyr442Oζ to Trp432Nε1. In this new conformation, Tyr442 is stabilized mainly by hydrophobic interactions with Phe423 and Phe446 and by an H-bond to a water molecule. The conformational change in the side chain of Tyr442 displaces Ala427, leading to shifts in main- and side-chain atoms from Arg426 to Val431. The narrowest dimension of the channel is characterized by a surface-to-surface distance of 3.4 Å, calculated using the programme HOLE.[13] Inspection of all 78 *Tc*AChE structures deposited in the PDB revealed only one other case (accession code 1HBJ[14]) in which Tyr442 adopts a very similar alternate conformation [Supporting Information Fig. S2(C)]. In 1HBJ, the enzyme was crystallized in a trigonal space group ($P3_121$; one monomer in the asymmetric unit), and the ligand, 4-amino-5-fluoro-2-methyl-3-(3-trifluoro-acetylbenzylthiomethyl)-quinoline (AFM-Q), was seen to occupy the "anionic" subsite of the active site (catalytic anionic site). In the AFM-Q/*Tc*AChE complex, the backdoor channel is slightly wider [Supporting Information Fig. S2(A); smallest surface-to-surface distance 3.5 Å] than that in the AB1/*Tc*AChE complex.

The alternate Tyr442 conformation seen experimentally was also observed transiently in a set of 10 20-ns MD simulations based on native *Tc*AChE (PDB entry code 1EA5, space group $P3_121$; see Supporting Information). The χ_1 and χ_2 angles reflecting

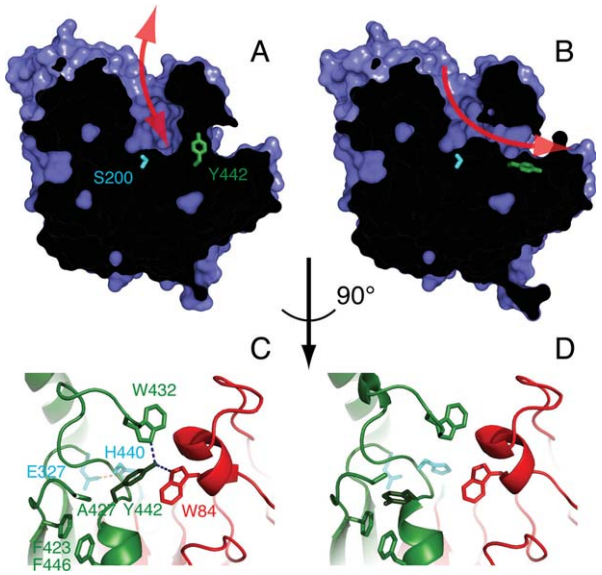

Figure 1. Backdoor in *Tc*AChE. A section (black) through the enzyme and its accessible surface area (blue) show (A) the catalytic serine (light blue; Ser200) at the bottom of the deep gorge and Tyr442 (green) in the native enzyme; (B) the opening of a backdoor in an aflatoxin/*Tc*AChE complex due to rotation of Tyr442 in monomer A. Tyr442Oζ is H-bonded to Trp84Nε1 within the ω-loop and to Trp432Nε1 in the native structure (C) but not in the complex (D). The red arrows in panels A and B suggest entrance and exit pathways for substrates and products, respectively.

the Tyr442 side-chain conformations accessed during the simulations include those observed in both 1HBJ and in 2XI4 monomer A (Fig. 2). Individual inspection revealed that the experimentally observed alternate Tyr442 conformation is accessed in only two of the 10 20-ns simulations (Supporting Information Fig. S3). The simulated Tyr442 conformations with χ_1 and χ_2 angles between 150° and 210°, and between 15° and 75°, respectively, correspond to 2.5% of the conformations accessed during the entire 200-ns simulation period (Fig. 2), which provides an idea of the frequency at which a Tyr442 conformation similar to the one observed in 2XI4 and 1HBJ is accessed. Neither the program Ringer,[15] nor the qFit WEB server,[16] found any evidence for an alternate conformation of Tyr442 in the crystal structure of the native enzyme (1EA5) similar to that in 2XI4. Similarly, Ringer did not detect evidence of an alternate conformation for Tyr442 in the aflatoxin complex structure (2XI4). Visual inspection suggested the presence of a native conformation in monomer A that may be populated to a very small level. Therefore, the occupancy of the primary conformation of Tyr442 was set to 80%. There was no visual evidence for an alternate conformation of Tyr442 in monomer B. We conclude that the crystallographically observed alternate Tyr442 conformation in monomer A of 2XI4 is part of the complex energy landscape of the native enzyme, even though it is rarely accessed.

We have recently used MD simulations to explore the exit pathways of the enzymatic hydrolysis product, thiocholine (TCh), from the active site of *Tc*AChE.[17] The crystal structure of a complex in which TCh was bound to *Tc*AChE at both the active site and the PAS (PDB entry code 2C5G[18]) served as the starting model for these simulations, with a total simulation time of 2.8 μs. The pathway most frequently taken by TCh to exit the active site was through a backdoor (see Ref. [17] for details). Detailed examination of the trajectory of exit of TCh via this route revealed that it involved a conformational change in Trp84 with concomitant breaking of the H-bond between Tyr442Oζ and Trp84Nε1 (Fig. 3).

The breaking of the Tyr442Oζ-Trp84Nε1 H-bond associated with the conformational change in Tyr442 observed in monomer A of 2XI4 may result in increased flexibility of the ω-loop [displayed in red in Fig. 1(C,D) and Supporting Information Fig. S2(C,D)], thus permitting the backdoor to open more widely. To explore this hypothesis, 10 20-ns MD simulations were performed based on the 2XI4 structure from which aflatoxin had been omitted (see Supporting Information). A snapshot from that simulation shows that Tyr442Oζ and Trp84Nε1 can move as far as 21.5 Å from each other [see Supporting Information Fig. S2(D) and magenta model in Fig. 4(A)], reflecting a large movement of the ω-loop that can occur when the Tyr442Oζ-Trp84Nε1 H-bond is broken. Analysis of the distribution of Tyr442Oζ-Trp84Nε1 distances in the course of the MD

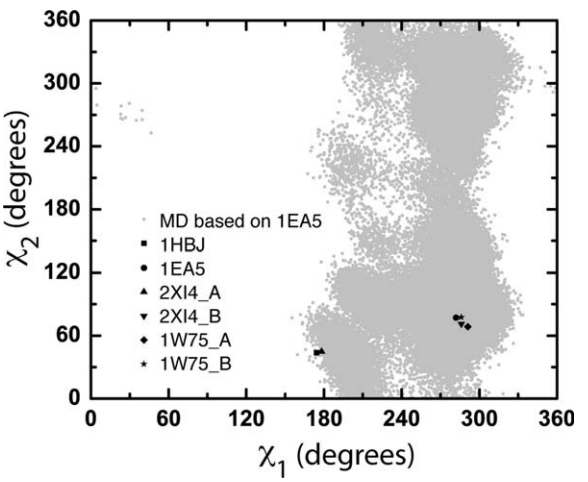

Figure 2. χ_1 and χ_2 angles of Tyr442 side-chain conformations from simulation and X-ray crystallography. Conformations from 10 20 ns-MD trajectories of native *Tc*AChE (PDB entry code 1EA5) are represented as grey dots, derived from snapshot structures extracted at 1 ps intervals (a total of 200,000). The triangle, inverted triangle, square, circle, diamond, and pentacle represent the conformations in the corresponding crystal structures. The Tyr442 conformation in monomer A of 2XI4 and in 1HBJ is accessed in the MD simulations of the native enzyme and is thus part of its complex energy landscape.

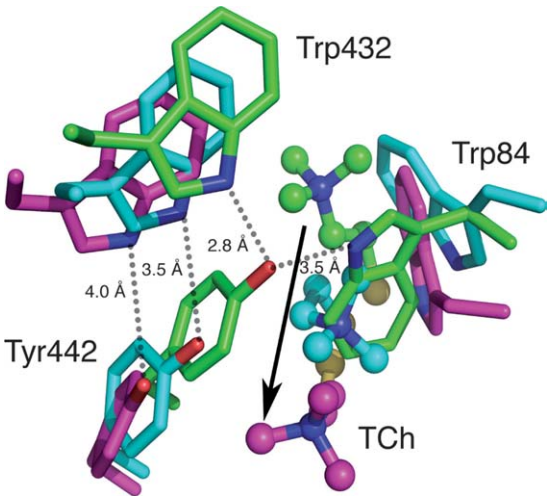

Figure 3. Positions of the side chains of Trp84, Trp432 and Tyr442, and of TCh taken from the crystal structure of the $(TCh)_2$/*Tc*AChE complex (PDB entry code 2C5G[18]) (green) and from snapshots extracted from an MD simulation of the complex at 4.2 ns (cyan) and 17.1 ns (magenta), which corresponds to simulation group III in Ref. 17. The distance between Tyr442Oζ and Trp84Nε1 in the crystal structure and the distances between Tyr442Oζ and Trp432Nε1 in the crystal structure and in the two MD snapshots are indicated. The arrow emphasizes the path taken by TCh to exit the enzyme through the backdoor.

simulations, based on 1EA5 and 2XI4 (Fig. 4B), indicates that the two atoms are on average much farther away from each other if the corresponding H-bond is already broken when the simulation commences (as in the simulations based on 2XI4) than when it is present (as in the simulations based on 1EA5). It should be noted that the peak at 16.5 Å in the distance distribution of simulations based on 1EA5 (green graph in Fig. 4B) corresponds to Tyr442 conformations close to the one observed in 2XI4 and 1HBJ. A large Tyr442Oζ-Trp84Nε1 distance such as the one depicted in Supporting Information Figure S2(D) and in the magenta model in Fig. 4(A) produces a backdoor with a smallest surface-to-surface distance of 5.7 Å. Most importantly, the snapshot depicted in Supporting Information Figure S2D and Figure 4(A) leads to sealing of the active-site gorge with concomitant opening of a backdoor [Supporting Information Fig. S2(B)] much more voluminous than that created by the movement of Tyr442 observed in monomer A of 2XI4 [Fig. 1(B)]. A sealed gorge might desolvate the substrate in the active site and increase catalytic efficiency as discussed earlier.[18]

The crystal structure presented, and the related MD simulations, terminate the long-standing controversy concerning the existence of a backdoor in AChE and shed light on the dynamic events accompanying catalysis by this rapid enzyme. The backdoor for whose existence we have now provided unequivocal experimental evidence provides a plausible route for the rapid clearance of the hydrolysis products from the active site. At the heart of the backdoor mechanism is a single H-bond that is linking the side chains of Tyr442 and Trp84 in the two subdomains of *Tc*AChE. If this H-bond is broken, either due to the movement of Tyr442 seen in the 2XI4 crystal structure, or by the movement of Trp84 detected by MD simulations[17] and kinetic crystallography,[11,19] a backdoor channel opens (Fig. 1B). This channel can be considerably enlarged through large-amplitude motions in the ω-loop, which can only occur after the H-bond between Trp84 and Tyr442 has snapped, as shown in the MD simulations (Supporting Information Fig. S2(B,D)]. The characterization of a new conformational substate of AChE, in which the alternate conformations of Tyr442 and of its close environment allow an alternative access route to the active-site gorge, allows better rationalization of the residual catalytic activity observed for AChE in its complex with the mamba venom neurotoxin, fasciculin,[7] which is known to cap the active-site gorge.[20,21] It also provides a new template for the rational design of AChE inhibitors and reactivators,

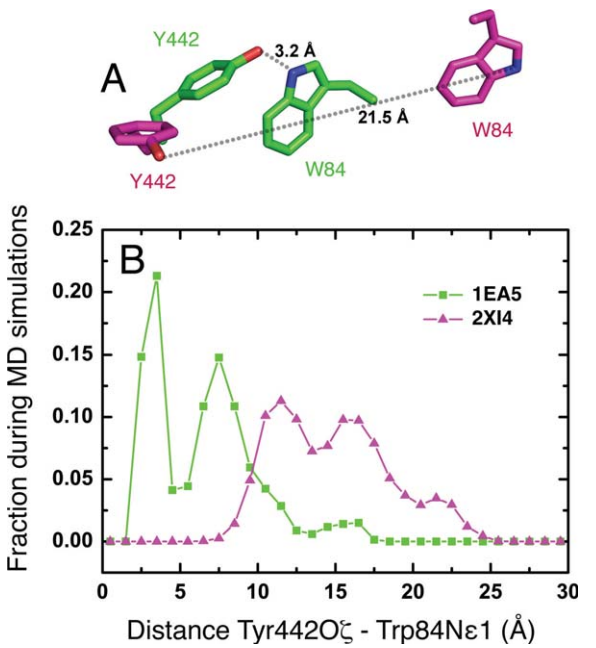

Figure 4. Distance between Tyr442Oζ and Trp84Nε1. (A) Orientations of Tyr442 and Trp84 in the crystal structure of native *Tc*AChE (green; PDB entry code 1EA5), and in a conformational snapshot taken 12 ns after initiation of one of the 10 20-ns MD trajectories of monomer A in the aflatoxin/*Tc*AChE complex (magenta; PDB code 2XI4) from which aflatoxin had been omitted. The orientation of the residues is similar to that in Figure 1(C,D) and Supporting Information Figure S2(C,D). (B) Histograms of distances between Tyr442Oζ and Trp84Nε1 based on snapshots extracted from the MD trajectories at 1-ps intervals. Each histogram is constructed making use of 200,000 data points and a bin size of 1 Å.

including anti-Alzheimer drugs and antidotes against organophosphate poisoning, respectively.

Acknowledgment

We warmly thank Henry van den Bedem for his help with qFit and Lilly Toker for the preparation of *Tc*AChE. We are grateful to the ESRF for beam-time under long-term projects MX498, MX609 and MX722 (IBS BAG) and MX551 and MX 666 (radiation-damage BAG) and to the ESRF staff for providing efficient help during data collection. We thank the European Commission VI Framework Research and Technological Development Program, "SPINE2-COMPLEXES" Project, under contract No. 031220, and "Teach-SG" Project, under contract No. ISSG-CT-2007-037198, the Kimmelman Center for Biomolecular Structure and Assembly, the Benoziyo Center for Neurosciences, the Nalvyco Foundation, the Bruce Rosen Foundation, the Jean and Julia Goldwurm Memorial Foundation. J.L.S. is the Morton and Gladys Pickman Professor of Structural Biology. J.P.C. is recipient of the International Young Researcher fellowship from the Chinese Academy of Science.

References

1. Silman I, Sussman JL (2005) Acetylcholinesterase: 'classical' and 'non-classical' functions and pharmacology. Curr Opin Pharmacol 5:293–302.
2. Sussman JL, Harel M, Frolow F, Oefner C, Goldman A, Toker L, Silman I (1991) Atomic structure of acetylcholinesterase from *Torpedo californica*: a prototypic acetylcholine-binding protein. Science 253:872–879.
3. Ripoll DR, Faerman CH, Axelsen PH, Silman I, Sussman JL (1993) An electrostatic mechanism for substrate guidance down the aromatic gorge of acetylcholinesterase. Proc Natl Acad Sci USA 90: 5128–5132.
4. Gilson MK, Straatsma TP, McCammon JA, Ripoll DR, Faerman CH, Axelsen PH, Silman I, Sussman JL (1994) Open "back door" in a molecular dynamics simulation of acetylcholinesterase. Science 263:1276–1278.
5. Tai K, Shen T, Borjesson U, Philippopoulos M, McCammon JA (2001) Analysis of a 10-ns molecular dynamics simulation of mouse acetylcholinesterase. Biophys J 81: 715–724.
6. Wiesner J, Kriz Z, Kuca K, Jun D, Koca J (2010) Influence of the acetylcholinesterase active site protonation on omega loop and active site dynamics. J Biomol Struct Dynamics 28:393–403.
7. Marchot P, Khelif A, Ji YH, Mansuelle P, Bougis PE (1993) Binding of 125I-fasciculin to rat brain acetylcholinesterase. The complex still binds diisopropyl fluorophosphate. J Biol Chem 268:12458–12467.
8. Kronman C, Ordentlich A, Barak D, Velan B, Shafferman A (1994) The "back door" hypothesis for product clearance in acetylcholinesterase challenged by site-directed mutagenesis. J Biol Chem 269:27819–27822.
9. Faerman C, Ripoll D, Bon S, Le Feuvre Y, Morel N, Massoulie J, Sussman JL, Silman I (1996) Site-directed mutants designed to test back-door hypotheses of acetylcholinesterase function. FEBS Lett 386:65–71.
10. Bartolucci C, Perola E, Cellai L, Brufani M, Lamba D (1999) "Back door" opening implied by the crystal structure of a carbamoylated acetylcholinesterase. Biochemistry 38:5714–5719.
11. Colletier JP, Bourgeois D, Sanson B, Fournier D, Sussman JL, Silman I, Weik M (2008) Shoot-and-Trap: use of specific x-ray damage to study structural protein dynamics by temperature-controlled cryo-crystallography. Proc Natl Acad Sci USA 105:11742–11747.
12. Morel N, Bon S, Greenblatt HM, Van Belle D, Wodak SJ, Sussman JL, Massoulie J, Silman I (1999) Effect of mutations within the peripheral anionic site on the stability of acetylcholinesterase. Mol Pharmacol 55: 982–992.
13. Smart OS, Neduvelil JG, Wang X, Wallace BA, Sansom MS (1996) HOLE: a program for the analysis of the pore dimensions of ion channel structural models. J Mol Graph 14:354–360, 376.
14. Doucet-Personeni C, Bentley PD, Fletcher RJ, Kinkaid A, Kryger G, Pirard B, Taylor A, Taylor R, Taylor J, Viner R, Silman I, Sussman JL, Greenblatt HM, Lewis T (2001) A structure-based design approach to the development of novel, reversible AChE inhibitors. J Med Chem 44:3203–3215.
15. Lang PT, Ng HL, Fraser JS, Corn JE, Echols N, Sales M, Holton JM, Alber T (2010) Automated electron-density sampling reveals widespread conformational polymorphism in proteins. Protein Sci 19:1420–1431.
16. van den Bedem H, Dhanik A, Latombe JC, Deacon AM (2009) Modeling discrete heterogeneity in X-ray diffraction data by fitting multi-conformers. Acta Crystallogr D Biol Crystallogr 65:1107–1117.
17. Xu Y, Colletier JP, Weik M, Qin G, Jiang H, Silman I, Sussman JL (2010) Long Route or Shortcut? A molecular dynamics study of traffic of thiocholine within the active-site gorge of acetylcholinesterase. Biophys J 99: 4003–4011.
18. Colletier JP, Fournier D, Greenblatt HM, Stojan J, Sussman JL, Zaccai G, Silman I, Weik M (2006) Structural insights into substrate traffic and inhibition in acetylcholinesterase. EMBO J 25:2746–2756.
19. Colletier J-P, Royant A, Specht A, Sanson B, Nachon F, Masson P, Zaccai G, Sussman JL, Goeldner M, Silman I, Bourgeois D, Weik M (2007) Use of a 'caged' analogue to study the traffic of choline within acetylcholinesterase by kinetic crystallography. Acta Crystallogr Sect D 63:1115–1128.
20. Harel M, Kleywegt GJ, Ravelli RB, Silman I, Sussman JL (1995) Crystal structure of an acetylcholinesterase–fasciculin complex: interaction of a three-fingered toxin from snake venom with its target. Structure 3: 1355–1366.
21. Bourne Y, Taylor P, Marchot P (1995) Acetylcholinesterase inhibition by fasciculin: crystal structure of the complex. Cell 83:503–512.